VCU

Virginia Commonwealth University
VCU Scholars Compass

Electrical and Computer Engineering Publications | Dept. of Electrical and Computer Engineering

2004

Excitonic fine structure and recombination dynamics in single-crystalline ZnO

A. Teke
Virginia Commonwealth University

Ü. Özgür
Virginia Commonwealth University, uozgur@vcu.edu

S. Doğan
Virginia Commonwealth University

See next page for additional authors

Follow this and additional works at: http://scholarscompass.vcu.edu/egre_pubs

Part of the Electrical and Computer Engineering Commons

Teke, A., Özgür, Ü., Doğan, S., et al. Excitonic fine structure and recombination dynamics in single-crystalline ZnO. Physical Review B, 70, 195207 (2004). Copyright © 2004 American Physical Society.

Downloaded from

http://scholarscompass.vcu.edu/egre_pubs/16

This Article is brought to you for free and open access by the Dept. of Electrical and Computer Engineering at VCU Scholars Compass. It has been accepted for inclusion in Electrical and Computer Engineering Publications by an authorized administrator of VCU Scholars Compass. For more information, please contact libcompass@vcu.edu.

Authors
A. Teke, Ü. Özgür, S. Doğan, X. Gu, Hadis Morkoç, B. Nemeth, J. Nause, and H. O. Everitt

This article is available at VCU Scholars Compass: http://scholarscompass.vcu.edu/egre_pubs/16

Excitonic fine structure and recombination dynamics in single-crystalline ZnO

A. Teke,* Ü. Özgür, S. Doğan,† X. Gu, and H. Morkoç
Department of Electrical Engineering, Virginia Commonwealth University, Richmond, Virginia 23284, USA

B. Nemeth and J. Nause
Cermet, Inc., Atlanta, Georgia 30318, USA

H. O. Everitt
Department of Physics, Duke University, Durham, North Carolina 27708, USA
(Received 27 October 2003; revised manuscript received 13 February 2004; published 12 November 2004)

The optical properties of a high quality bulk ZnO, thermally post treated in a forming gas environment are investigated by temperature dependent continuous wave and time-resolved photoluminescence (PL) measurements. Several bound and free exciton transitions along with their first excited states have been observed at low temperatures, with the main neutral-donor-bound exciton peak at 3.3605 eV having a linewidth of 0.7 meV and dominating the PL spectrum at 10 K. This bound exciton transition was visible only below 150 K, whereas the A-free exciton transition at 3.3771 eV persisted up to room temperature. A-free exciton binding energy of 60 meV is obtained from the position of the excited states of the free excitons. Additional intrinsic and extrinsic fine structures such as polariton, two-electron satellites, donor-acceptor pair transitions, and longitudinal optical-phonon replicas have also been observed and investigated in detail. Time-resolved PL measurements at room temperature reveal a biexponential decay behavior with typical decay constants of ~170 and ~864 ps for the as-grown sample. Thermal treatment is observed to increase the carrier lifetimes when performed in a forming gas environment.

DOI: 10.1103/PhysRevB.70.195207 PACS number(s): 78.55.Et, 78.47.+p, 71.35.−y

I. INTRODUCTION

ZnO is a direct band gap semiconductor with optical properties similar to GaN. Many sharp near band edge photoluminescence (PL) lines at low temperatures are usually observed in high quality ZnO single crystals. Its high band gap energy of 3.37 eV at room temperature[1] and free-exciton binding energy of 60 meV[2,3] (much larger than that of GaN ~ 26 meV) along with its larger absorption coefficient compared to GaN make ZnO a potential candidate for optoelectronics applications, such as blue and ultraviolet (UV) light emitters and UV detectors.[4] The large exciton binding energy ensures that excitonic emission is significant at room temperature. Exciton related stimulated emission and optically pumped laser action in ZnO epitaxial films have been observed at room temperature.[5,6] The recent availability of large size high crystalline quality bulk ZnO can also be considered as an advantage not only for homoepitaxial ZnO growth, but also for GaN growth due to its potential as a suitable substrate with similar crystalline properties. ZnO is typically *n*-type and attempts to implement *p*-type doping have not been successful until recently.[7,8]

Although the progress towards the realization of device applications is fast, some fundamental issues related to the optical properties of ZnO are still under debate. The low temperature PL spectrum of ZnO single crystal has been investigated in many aspects by many researchers.[3,9–16] However, no consensus has been established for assignments of the various sharp emission peaks associated with either intrinsic or extrinsic transitions. Other than pointing at the discrepancies in the literature, a better understanding of the fine structure is necessary for further development of ZnO-based photonic and electrical devices. For device designs, knowledge of carrier recombination times is imperative, especially for operation at room temperature since almost all device operation is at or above room temperature.

In this study, we investigated the low temperature continuous wave (cw) PL spectrum of a high quality ZnO single crystal annealed in a forming gas environment. The assignments of the excitonic peaks are verified by reflectivity measurements, the temperature evolution of the particular PL transition, and comparison with literature. After reviewing the experimental details in the following section, we discuss different regions of the full PL spectrum, measured at 10 K, separately for the sake of simplicity. First, the intrinsic excitonic features in the 3.376–3.450 eV range are discussed. The spectral region corresponding to the donor and acceptor bound excitons is analyzed next. Then, two electron satellites related to the donor-bound excitons are investigated. Finally, longitudinal optical (LO)-phonon replicas of the main excitonic emissions and the donor-acceptor-pair transition (DAP) are identified. The temperature dependence of the full PL spectrum is also explored and necessary arguments are made to support the peak assignments. In addition, time-resolved PL spectroscopy is performed at room temperature to measure the recombination lifetimes both for the as received and the annealed samples to investigate the effects of the post treatment.

II. EXPERIMENT

Two high quality bulk ZnO single crystal samples of wurtzite structure produced by Cermet, Inc., one as received

1098-0121/2004/70(19)/195207(10)/$22.50 ©2004 The American Physical Society

and the other subjected to post thermal treatment, were used in this study. For post treatment, we annealed the ZnO sample in a forming gas environment (5% H_2 and 95% N_2) at 600 °C for 10 min in a conventional quartz tubular annealing furnace. The post treatment is observed to strengthen the intrinsic excitonic features significantly due to the improvement of crystal quality at the surface. Therefore, for clarity only the analysis associated with the post treated sample is reported for steady state PL and reflectivity measurements, whilst time-resolved PL data are presented for both samples to underscore the importance of surface treatment.

Steady-state photoluminescence and reflectivity measurements were carried out with the samples placed in a close-cycled cryostat in the temperature range of 10–300 K. As an excitation source, a 25 mW, 325 nm He-Cd laser was used for PL, and a 30 W deuterium lamp was used for reflectivity measurements. The luminescence or the reflected light collected by suitable lenses was then dispersed by a 1250 mm monochromator and detected by a photomultiplier tube in a standard photon counting mode. Narrow (<10 μm) monochoromator slits were used to achieve better resolution. The wavelength calibration was verified with standard lines from a mercury calibration lamp. The overall resolution of the experimental setup was better than 0.2 meV.

For time-resolved measurements, the samples were excited at a 45° angle by 325 nm, ~100 fs, ~10 μJ pulses from a 1 kHz repetition rate optical parametric amplifier. The laser was focused to a spot size of ~1 mm and excitation density dependence was investigated using neutral density filters for attenuation. PL was collected perpendicular to the surface using an ultraviolet optical fiber. A Hamamatsu streak camera with a system resolution of ~50 ps was used to measure the time-resolved PL (TRPL).

III. FREE EXCITONS AND POLARITONS

The optical properties of a semiconductor are connected with both intrinsic and extrinsic effects. Photoluminescence measurement is a suitable tool to determine the crystalline quality and the presence of impurities in the material as well as exciton fine structures. The wurtzite ZnO conduction band is mainly constructed from the *s*-like state having (Γ_7^c) symmetry, whereas the valence band is a *p*-like state, which is split into three bands due to the influence of crystal field and spin-orbit interactions.[17] However, the ordering of the crystal-field and spin-orbit coupling split states of the valence-band maximum in wurtzite ZnO has been a subject of controversy.[3,17–20] The difference arises from the interpretation of the spectral line, which was assigned to intrinsic ground state A-exciton transition by Thomas,[18] and contrarily to extrinsic, ionized donor-bound exciton complex transition by Park *et al.*[19] Recent availability of high quality ZnO single crystals has enabled researchers to observe intrinsic exciton transitions in low temperature photoluminescence and magnetoluminescence measurements.[3,11,12] Reynolds *et al.*[3] addressed this issue using second-order photoluminescence spectra, which helped resolve the additional fine structure of the excitons. They concluded that the valence-band symmetry ordering (A-Γ_9, B-Γ_7, and C-Γ_7) in ZnO is not reversed but the same as that observed in most other wurtzitic II–VI structures and GaN.

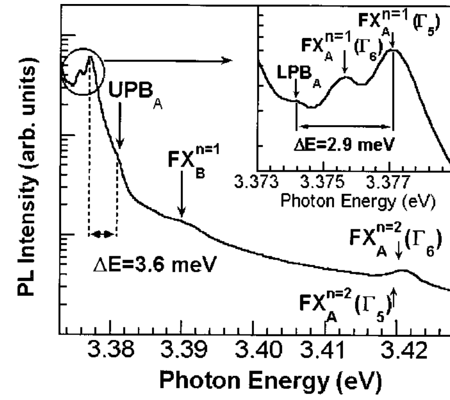

FIG. 1. Free excitonic fine structure region of the 10 K PL spectrum for the forming gas annealed ZnO substrate.

Group theoretical arguments and the direct product of the group representations of the band symmetries (Γ_7 for the conduction band, Γ_9 for the A valence band, upper Γ_7 for the B valence band, and lower Γ_7 for the C valence band) will result in the following intrinsic exciton ground state symmetries:

$$\Gamma_7 x \Gamma_9 \rightarrow \Gamma_5 + \Gamma_6, \quad \Gamma_7 x \Gamma_7 \rightarrow \Gamma_5 + \Gamma_1 + \Gamma_2.$$

The Γ_5 and Γ_6 exciton ground states are both doubly degenerate, whereas Γ_1 and Γ_2 are both singly degenerate. Γ_5 and Γ_1 are allowed transitions with $\mathbf{E} \perp \mathbf{c}$ and $\mathbf{E} \parallel \mathbf{c}$, respectively, but the Γ_6 and Γ_2 are not allowed.

Figure 1 shows the PL spectrum in the range of fundamental excitonic region measured at 10 K in the $\mathbf{E} \perp \mathbf{c}$ polarization geometry for a high quality ZnO crystal annealed in forming gas. The A-free exciton and its first excited state emission are observed at $FX_A^{n=2}=3.3771$ eV (3.3757 eV for Γ_6) and $FX_A^{n=1}=3.4220$ eV for Γ_5 (3.4202 eV for Γ_6) band symmetry, respectively. Although, at $k=0$, Γ_6 exciton is forbidden in the current measurement mode of polarization, it is still seen, evidently due to the fact that the photon has finite momentum. Geometrical effects such as not having the sample orientation exactly perpendicular to the electric field can also be considered as a reason for the observed Γ_6 transition. Using the energy separation of ground state and excited state peak positions, and assuming that exciton has a hydrogen-like set of energy levels, the exciton binding energy and band gap energy can be predicted. The energy difference of about 45 meV gives an A-free exciton binding energy of 60 meV and a corresponding band gap energy of 3.4371 eV at 10 K. Based on the reported energy separation of the A- and B-free excitons (in the range of 9–15 meV),[3,12,18] we assigned the weak emission centered at 3.3898 eV, which is about 12.7 meV apart from the A exciton, to the B exciton transition.

Additional fine structure of exciton lines was also observed in low temperature PL spectra. In strongly polar materials like ZnO transverse Γ_5 excitons couple with photons to form polaritons. In principle, although the polaritons can be formed anywhere along the dispersion curves, polariton

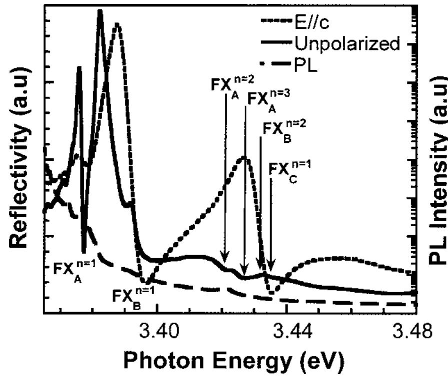

FIG. 2. Reflection spectra of the forming gas annealed ZnO substrate measured at 10 K with unpolarized light and with $E//c$. The PL spectrum is also superimposed for comparison.

lifetimes, which are higher at certain points, determine the observed peak positions. Therefore, as indicated in Fig. 1, the $FX_A^{n=1}$ (Γ_5) exciton line has two components. The higher energy component at 3.3810 eV, which is 3.6 meV apart from the A exciton, can be assigned to the so-called longitudinal exciton (upper polariton branch—UPB_A). The lower energy component at 3.3742 eV, which is about 2.9 meV apart from the A exciton, corresponds to the recombination from the "bottleneck" region, in which the photon and free-exciton dispersion curves cross (lower polariton branch—LPB_A). These assignments are also consistent with the theory used to calculate the energy separation between the main exciton and the polariton branches. The longitudinal-transverse energy splitting is given by $\Delta E = E(\Gamma_5)4\pi\alpha/2\varepsilon$, where $E(\Gamma_5)$ is the energy of the Γ_5 exciton, $4\pi\alpha$ is the polarizability, and ε is the optical dielectric constant. By using the reported values of 7.7×10^{-3} for polarizability[21] and 4.0–5.0 for optical dielectric constant,[22,23] the calculated value remains in the range of 2.6–3.3 meV for $E(\Gamma_5) = 3.3771$ eV. The measured energy splitting (2.9 meV for LPB_A and 3.6 meV for UPB_A) is comparable to the predicted values, supporting the assignment of these two peaks. Since Γ_6 excitons do not have transverse character, they do not interact with light to form polaritons, and thus have only normal free-exciton dispersion curves as seen in the PL spectra.

Low temperature reflectivity measurements were also performed in order to validate the free excitonic features and corresponding peak assignments discussed above. In ideal, i.e., strain free, wurtzite crystals A, B, and C exciton states obey the following selection rules in optical one-photon processes: all excitons are allowed in the σ polarization ($\mathbf{E}\perp\mathbf{c}$ and $\mathbf{k}\perp\mathbf{c}$ axis), but the C exciton is quite weak. The C exciton is strongly allowed in the π polarization ($\mathbf{E}\|\mathbf{c}$ and $\mathbf{k}\perp\mathbf{c}$); however, the A exciton is forbidden and the B exciton is only weakly observable. In the α polarization ($\mathbf{E}\perp\mathbf{c}$ and $\mathbf{k}\|\mathbf{c}$) all three transitions are clearly observable. Figure 2 shows reflectivity measurements performed at 10 K for unpolarized and π polarized light. The 10 K PL spectrum is also superimposed on the same graph to show the agreement in the peak positions. For unpolarized light, ground and first excited states of A and B excitons along with a weak C-exciton feature are observed. The reflection minima at $FX_A^{n=1} = 3.3772$ eV and $FX_B^{n=1} = 3.3901$ eV are in excellent agreement, within the experimental resolution, with the emission peaks for A- and B-free excitons in PL spectra. The position of the first excited state ($FX_A^{n=2} = 3.421$ eV) and the binding energy of the A-free exciton ($\sim$60 meV) were also confirmed by reflectivity measurements. Additionally, the reflection minima at 3.427 and 3.433 eV are assumed to be related to the second and the first excited states of the A- and B-free excitons, respectively. For $E//c$ polarized light, C exciton at 3.435 eV is more pronounced. As will be discussed later, the temperature evolutions of the A and B exciton PL peaks also reveal characteristic features related to these excitonic transitions supporting this premise.

Table I tabulates the excitonic peak energies observed in this study along with the recently reported results for high quality ZnO single crystals. The peak position of the A- and B-free excitons, and the first excited states of the A exciton are in very good agreement, within the experimental accuracy, with the results reported by Reynolds *et al.*[3] The observed polariton positions are also in reasonable agreement with the reported energies for bulk ZnO grown by Eagle-Picher using vapor-phase-transport method. Even though the current study does not provide any direct evidence for the valence band ordering conflict, it does provide a level of confidence in the identification of the position of excitonic fine structures in high quality bulk ZnO. However, it should be noted that experimental resolution and the wavelength calibration of the particular spectrometer used must be considered carefully to identify the exact peak positions of the very narrow excitonic lines.

TABLE I. Excitonic peak energies (eV) in ZnO single crystals.

	$FX_A^{n=1}$ (Γ_5)	$FX_A^{n=1}$ (Γ_6)	$FX_A^{n=2}$ (Γ_5)	$FX_A^{n=2}$ (Γ_6)	LPB_A	UPB_A	$FX_B^{n=1}$
Present work	3.3771	3.3757	3.4220	3.4206	3.3740	3.3810	3.3898
Reynolds *et al.*[a]	3.3773	3.3756	3.4221	3.4209			3.3895
Reynolds *et al.*[b]	3.3793	3.3775			3.3743	3.3829	
Chichibu *et al.*[c]	3.378				3.3768	3.3783	3.386
Hamby *et al.*[d]	3.378				3.374		3.385

[a]See Ref. 3.
[b]See Ref. 16.
[c]See Ref. 24.
[d]See Ref. 14.

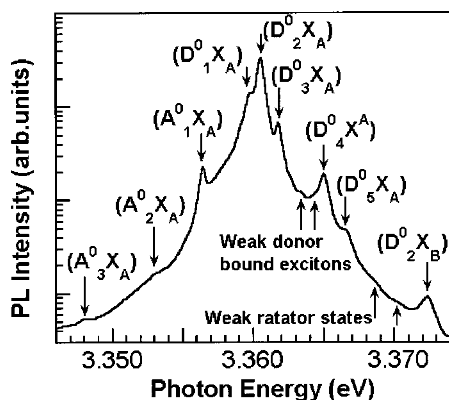

FIG. 3. Bound excitonic region of the 10 K PL spectrum for the forming gas annealed ZnO substrate.

IV. BOUND EXCITONS

Extrinsic properties are related to dopants or defects, which usually create discrete electronic states in the band gap, and therefore influence both optical absorption and emission processes. Bound excitons fit in this category and the electronic states of the bound excitons depend strongly on the semiconductor material, in particular the band structure. In theory, excitons could be bound to neutral or charged donors and acceptors. A basic assumption in the description of the bound exciton states for neutral donors and acceptors is a dominant coupling of the like particles in the bound exciton states.[25] These two classes of bound excitons are by far the most important cases for direct band gap materials. In high quality bulk ZnO substrates, the neutral shallow donor-bound exciton (DBE) often dominates because of the presence of donors due to unintentional impurities and/or shallow donor-like defects. In samples containing acceptors, the acceptor-bound exciton (ABE) is observed. The recombination of bound excitons typically gives rise to sharp lines with a photon energy characteristic to each defect. Many sharp donor- and acceptor-bound exciton lines were reported in the narrow energy range from 3.348 to 3.374 eV in ZnO (see for example Ref. 26, and references therein). However, the chemical origin and binding energy of the most underlying donor and acceptor atoms remain unclear.

The low-temperature PL spectra are dominated by several bound excitons in the range from 3.348 to 3.374 eV for our bulk ZnO sample, as seen in Fig. 3. The prominent lines are the A excitons bound to neutral donors that are positioned at 3.3598 $(D^0{}_1X_A)$, 3.3605 $(D^0{}_2X_A)$, 3.3618 $(D^0{}_3X_A)$, 3.3650 $(D^0{}_4X_A)$, and 3.3664 $(D^0{}_5X_A)$ eV. The most intense peak at 3.3605 has a full width at half maximum of about 0.7 meV, indicating the good quality of the sample. Several small peaks and shoulders are also observed between these prominent lines. Based on the energy separation between the $FX_A^{n=1}$ (Γ_5) and the DBE peaks, we concluded that the binding energies of the DBEs related to the different donors range from 10 to 20 meV.

On the high-energy side of the neutral DBE, transitions between 3.3664 and 3.3724 eV have been attributed to the excited states or excited rotator states of the neutral-donor-bound excitons. These excited states are analogous to the rotational states of the H_2 molecule. Several models were proposed to explain the rotator states for different material systems. To identify these rotator states in bulk ZnO, Reynolds *et al.*[9] adopted the model, which is originally proposed by Rarison *et al.*[28] to explain their high magnetic field results in InP. In this model, DBEs are considered to be free excitons rotating around neutral donors, where one electron of the DBE state is strongly correlated with the hole and the other with the donor. In Ref. 9, the transitions observed at 3.3662 (Γ_6) and 3.3670 (Γ_5) eV were attributed to the rotator states associated with the ground state neutral bound exciton line at 3.3564 eV. The peaks at 3.3702 (Γ_6) and 3.3714 eV (Γ_5) are assigned to the rotator states of the neutral bound exciton at 3.3594 eV. In our measurements, very weak emissions at 3.3686 (Γ_6) and 3.3702 (Γ_5) eV with an energy separation of about 1.6 meV have been attributed to the rotator states associated with the main neutral bound exciton emission at 3.3605 eV $(D^0{}_2X_A)$. The splitting of these two peaks is consistent with the energy separation of the Γ_6 and Γ_5 band symmetries. We also observed the relatively strong emission line at 3.3724 eV $(D^0{}_2X_B)$ that is attributed to the transition due to the B-free exciton bound to the same main neutral donor. The energy separation between this peak and the main peak at 3.3605 eV $(D^0{}_2X_A)$ is about 12 meV, which is consistent with the energy splitting of the A- and B-free exciton lines. Analyzing the temperature dependence of the PL spectrum will also support this assignment. In the lower energy part of the PL spectrum, ABEs at 3.3564 $(A^0{}_1X_A)$, 3.3530 $(A^0{}_2X_A)$, and 3.3481 eV $(A^0{}_3X_A)$ are also observed.

The bound exciton peak energies in our ZnO sample together with the recently reported values observed in low temperature PL are given in Table II for comparison. Reynolds *et al.*[9] have investigated the bound-exciton region in detail by using low temperature PL measurements performed at different modes of polarizations and applied magnetic fields. They resolved seven bound-exciton lines using the second-order grating configuration in the bound exciton spectral region. However, as we mentioned before, wavelength calibration is particularly important to determine the position of the sharp lines. In this particular paper there is almost a 2 meV shift between the first- and the second-order PL spectra that might be due to experimental issues associated with the spectrometer used. Nevertheless, the peak energies of the neutral DBEs in our bulk ZnO sample are almost at the same positions, within the experimental resolution, as those reported by Reynolds *et al.*[9] However, relative peak intensities of the particular donor-related exciton lines show some differences from sample to sample. For example, the most intense line was observed at 3.3628 eV by Thonke *et al.*,[11] at 3.3624 eV by Reynolds *et al.*,[9] at 3.3653 eV by Boemare *et al.*,[12] and at 3.364 eV by Alves *et al.*[15] and Hamby *et al.*,[14] whereas we observed the most intense neutral DBE line at 3.3605 eV. This is because the concentration of the particular donor could vary from sample to sample as well as its capture cross section.

In the ABE region, the main peak at 3.3564 eV is commonly observed by others and is probably related to the Na or Li acceptors.[27] Other two weak emissions at 3.3481 and

TABLE II. Bound exciton peak energies (eV) in ZnO single crystals.

	Neutral acceptor bound excitons			A excitons bound to neutral or ionized donors						Rotator states		B excitons bound to neutral donor
Present work	3.3481	3.3530	3.3564	3.3598	3.3605	3.3618	3.3634	3.3650	3.3664	3.3686	3.3702	3.3724
							3.3643					
Reynolds *et al.*[a]			3.3562	3.3594	3.3602	3.3610	3.3624	3.3652		3.3670	3.3702	
							3.3634			3.3664	3.3714	
Alves *et al.*[b]			3.358		3.361	3.362		3.364				
Thonke *et al.*[c]			3.3566	3.3597	3.3606	3.3620	3.3628	3.364				
Boemare *et al.*[d]				3.3592			3.3622	3.3653	3.3693	3.3693	3.3741	3.3707
							3.3632			3.3707	3.3754	3.3741
												3.3754
												3.3772

[a]See Ref. 9.
[b]See Ref. 15.
[c]See Ref. 11.
[d]See Ref. 12.

3.3530 eV are also seen, which indicates the presence of the deeper acceptor states in our ZnO sample. However, their chemical origin has not yet been identified.

V. TWO-ELECTRON SATELLITES

Another characteristic of the neutral-donor-bound exciton transition is the two-electron satellite (TES) transitions in the spectral region of 3.32–3.34 eV. These transitions involve radiative recombination of an exciton bound to a neutral donor, leaving the donor in the excited state. In the effective-mass approximation, the energy difference between the ground-state neutral DBEs and their excited states (TES) can be used to determine the donor binding energies[11,15] (the donor excitation energy from the ground state to the first excited state equals to 3/4 of the donor binding energy, E_D) and catalog the different species present in the material. The spectral region for the expected two-electron satellite transitions is shown in Fig. 4 for the forming gas annealed ZnO sample. The main peak at 3.3224 eV $(D^0{}_2X_A)_{2e}$ is the excited state associated with the most intense neutral DBE at 3.3605 eV $(D^0{}_2X_A)$. The shoulder seen at about 3.3268 eV $(D^0{}_3X_A)_{2e}$ on the high-energy side of the main TES peak is related to the excited state of the donor whose ground state emission is at 3.3618 eV $(D^0{}_3X_A)$. A weak emission at 3.3364 eV $(D^0{}_4X_A)_{2e}$ is also attributed to the TES transition of the neutral donor whose ground state is at 3.3650 eV $(D^0{}_4X_A)$. From the separation of the ground state and the corresponding excited states, we were able to calculate the donor binding energies as 51 meV for the donor at 3.3606 eV, 47 meV for the donor at 3.3618, and 38 meV for the donor at 3.3650 eV.

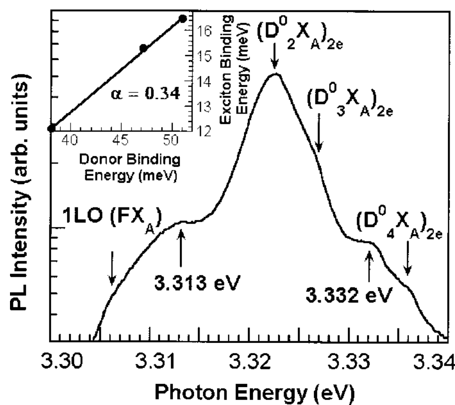

FIG. 4. 10 K PL spectrum for the forming gas annealed ZnO substrate in the TES region of the main bound exciton lines. Inset shows the exciton binding energy vs donor binding energy.

From the separation between the A-free exciton and the ground-state neutral DBEs, we can also determine the binding energies of these excitons as 16.5 meV (for 3.3605 eV), 15.3 meV (for 3.3618 eV), and 12.1 meV (for 3.3560 eV). According to the empirical Haynes rule, the binding or localization energy of the DBEs is proportional to the binding energy of the corresponding donor. Indeed, this relation is clearly seen in the inset of Fig. 4. The proportionality constant (α) is found to be 0.34, which is close to the 0.3 reported by Alves *et al.*,[15] who calculated the binding energies of the donors as 43, 52, and 55 meV for the donors whose ground state bound exciton lines are at 3.364, 3.362, and 3.361 eV, respectively. Supporting our findings is another study on TES by Thonke *et al.*[11] They found the binding energies of two shallow donors to be 39.9 and 55.5 meV. Reynolds *et al.*[9] reported two donor binding energies of 55.5 and 56.7 meV for donors at 3.3636 and 3.3614 eV, respectively. The Haynes proportionality constant obtained from these binding energies is about 2, much higher than the values given above. There are two additional peaks at 3.332 and 3.312 eV on both sides of the main TES lines, which could not be identified at this point, but they may be related to the excitons bound to structural defects.

VI. DAP AND LO-PHONON REPLICAS

The spectral region containing the DAP transition and LO-phonon replicas of the main transitions has not been

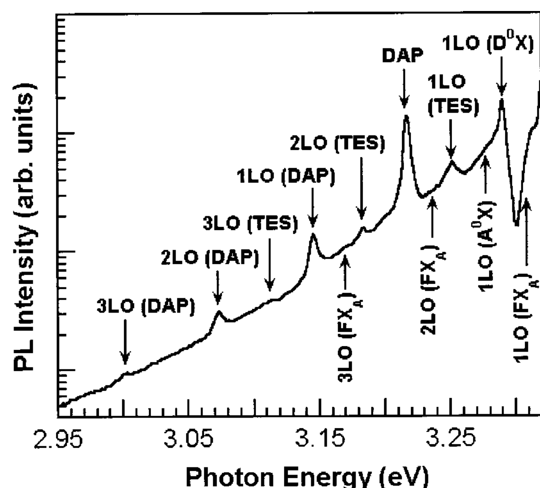

FIG. 5. 10 K PL spectrum for the forming gas annealed ZnO substrate in the region where donor-acceptor-pair transition and LO-phonon replicas are expected to appear.

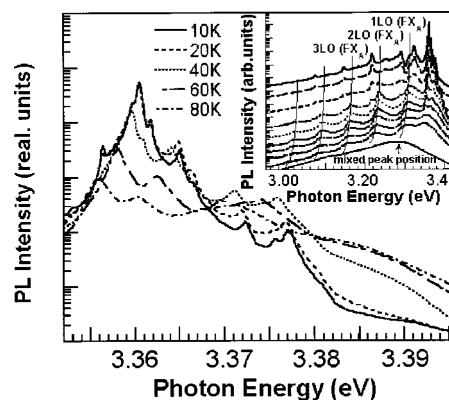

FIG. 6. Temperature dependent PL spectrum for the forming gas annealed ZnO substrate. The inset shows the PL in the DAP and LO-phonon replicas region up to 160 K. The spectrum for each temperature is displaced vertically for clarity. The room temperature PL data is also included at the bottom. The lines drawn on some peaks are for guidance.

studied widely for single crystal ZnO. Figure 5 shows the corresponding spectrum measured at 10 K for the forming gas treated sample. It should be noted that LO-phonon replicas occur with a separation of 71–73 meV, which corresponds to the LO-phonon energy in ZnO.[30] Since some of the peaks are either very weak or mixed with other closely spaced peaks, temperature evolution of these peaks should be tracked carefully in order to make sure that the corresponding assignments are correct. As indicated in Fig. 5, the bump at the higher energy side of the spectrum labeled as $1\text{LO}(FX_A)$ has a peak around 3.306 eV, which is the expected value for the 1LO-phonon replica of the free exciton peak (about 71 meV apart from the $FX_A^{n=1}$ free-exciton peak). Although weak, second and third order LO phonon replicas labelled as 2LO (FX_A) and 3LO (FX_A) are also observed in the PL spectrum.

The first order LO phonon replicas of the main neutral bound excitons should fall between 3.290 and 3.295 eV. However, due to the line broadening, the peaks corresponding to each individual bound exciton could not be resolved very well. Indeed, the peak labeled as $1\text{LO}(D^0X)$ has a linewidth of about 6 meV, which prevents a definitive resolution. LO-phonon replicas of the peak at 3.3650 eV can be separated from the two other closely spaced peaks at 3.3618 and 3.3605 eV. The peak at 3.2898 is the first LO-phonon replica of both 3.3618 and 3.3605 eV lines, whereas the first LO-phonon replica of 3.3650 eV line is seen as a shoulder on the high-energy side of this intense peak. Resolving the second and higher order LO replicas is even harder because the energy position (3.218–3.223 eV) falls in the spectral region where the DAP transition and its LO phonon replicas are expected to appear. In fact, we observed a radiative recombination peak at 3.217 eV that is attributed to the donor-acceptor-pair (labeled as DAP in Fig. 5 along with its first, second, and third LO-phonon replicas at 3.145, 3.073, and 3.001 eV, respectively). Regarding the origin of the emission line at 3.2898 eV, Reynolds *et al.*[10] argued that this line is related to the acceptor-associated transition based on their internal strain study by changing the postannealing temperatures, which disagrees with our interpretation. Although our investigation differs somewhat, we can resolve at least two closely spaced peaks at 3.2898 and 3.2920 eV, which are about 72 meV apart from the main neutral DBE lines at 3.3605 and 3.3650 eV. The temperature dependent measurements also show that relative intensities of these LO-phonon replicas follow those of the main bound excitons. Additionally, LO-phonon replicas are expected to be roughly two orders of magnitude less intense than the neutral DBE lines,[11] which is also the case in the current study. This is also similar to the case of GaN and other II–VI semiconductors, where donor-related bound exciton lines couple only weakly with the optical phonons.

The relatively broad peak around 3.280 eV is the first LO-phonon replica associated with the most intense ABE line (3.3564 eV). This is indicated as 1LO (A^0X) in Fig. 5. Finally, first, second, and third order LO-phonon replicas of the TES lines are also clearly observed in the PL spectra. These peaks are labeled as 1LO, 2LO, and 3LO (TES) and they are positioned at 3.252, 3.182, and 3.112 eV, respectively.

VII. TEMPERATURE DEPENDENT MEASUREMENTS

In order to support some of the peak assignments in the low temperature PL spectrum of the high quality ZnO substrate, we studied the temperature evolution of these peaks. The temperature dependent measurements were performed between 10 and 300 K, the results of which are shown in Fig. 6. The spectrum for each temperature is displaced vertically for clarity.

The variation of both A and B exciton peak positions with temperature is shown in the inset of Fig. 6. The A and B exciton peaks can be traced up to ~160 K, above which line broadening prevents a proper distinction among the two. This is clearly seen for the room temperature PL spectrum, where the peak position is at ~3.28 eV instead of the expected position of 3.31 eV (if we use the mostly accepted

band gap of 3.37 eV[1] and the measured 60 meV binding energy). As the temperature is increased, the convergence of the A and the B excitons and the 1 LO-phonon replica coupled with line broadening of each of these peaks hampers the accurate determination of the peak positions above 160 K. Therefore, the room temperature peak should be considered a combination of these multiple peaks.

The intensity of A- and B-free excitons increase with temperature up to 40 and 80 K, respectively, and then decrease as the temperature is increased further. From this observation, we can attribute the 3.3771 and 3.3898 eV emission lines at 10 K (as discussed before) to the free excitons corresponding to the A and the B bands, respectively. The most intense ABE peak at 3.3564 eV $(A^0{}_1X_A)$ quenches gradually with increasing temperature as well as the other two weak acceptor-related peaks labeled as $(A^0{}_2X_A)$ and $(A^0{}_3X_A)$, and disappears above 40 K. The temperature evolution of the main neutral DBEs was also traced within the temperature range of 10–160 K (see also the Fig. 6 inset). With increasing temperature, the main peak related to $(D^0{}_2X_A)$ at 3.3605 eV and its TES along with their LO-phonon replicas quench. On the other hand, relative intensities of the bound exciton emissions lying between this main DBE peak and the A-free exciton peak increase initially, where the strength depends on the particular bound exciton, and then decrease at higher temperatures. The intensity of the bound exciton peak at 3.3724 eV, which was attributed to the B exciton bound to the main donor rather than to a rotator state, follows the temperature behavior of the B exciton up to 40 K supporting our assignment. Although the B-free exciton emission continues to increase until 80 K, further increase of the donor bound B exciton intensity is prevented due to its partial dissociation above 40 K. The observed temperature characteristics of the free and main bound exciton, where the relative intensity I_{FX}/I_{BX} is seen to increase with increasing temperature, can be interpreted using the approach of Viswanath *et al.*[29] for the study of GaN. They also observed an increase in this ratio and inferred that with increasing temperature the main DBE dissociates into a free exciton and a neutral donor. Based on this argument and the works of Reynolds *et al.*[9] and Hamby *et al.*,[14] we similarly conclude that thermal dissociation of the 3.3605 eV bound exciton results in increased emission from the free excitons and other shallower donor-bound excitons.

There is a controversy in the assignment of the 3.223 eV peak, which is close to the main DAP transition at low temperature. Analyzing its temperature dependence, Thonke *et al.*[11] attributed this peak to the free electron-acceptor (e,A^0) transition due to thermal ionization of the donor with increasing temperature. With the help of Hall measurements, they determined the acceptor ionization energy as $\sim$195 meV for the unintentional acceptor present in ZnO, the chemical origin of which was assumed to be the substitutional nitrogen on O sites. On the other hand, Hamby *et al.*[14] attributed this peak to the second LO-phonon replica of the A-free exciton. They observed a very good agreement in temperature dependent energy positions of this peak with the predicted values by taking into account the temperature broadening effect. In the current study, we also assign this

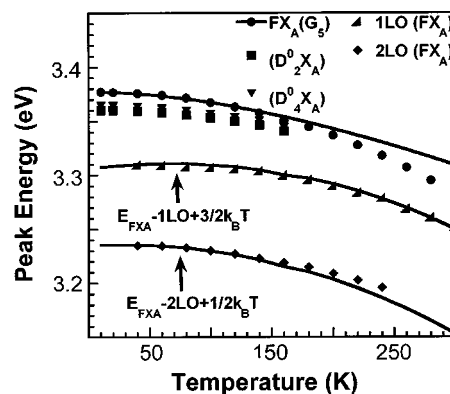

FIG. 7. Temperature dependent peak positions of the A-free exciton, $FX_A^{n=1}$ (Γ_5) and its 1LO- and 2LO-phonon replicas. Also shown are the temperature evolutions of the peak positions of two major neutral-donor bound exciton transitions at 3.3606 and 3.3650 eV. The $FX_A^{n=1}$ (Γ_5) data were fit using Varshni equation and LO-phonon replicas were fit with the equation shown in the figure.

peak to the 2LO phonon replica of the A-free exciton depending on its temperature evolution. As seen in Fig. 6, the main DAP line and its LO-phonon replicas quench with increasing temperature, while the adjacent line at 3.223 eV on the high energy side increases and becomes more apparent at higher temperatures. The temperature dependence of this peak is similar to the A-free exciton; it increases with increasing temperature up to 60 K and then decreases at higher temperatures. Also, by following the approach of Hamby *et al.*,[14] we plotted the variation of A-free exciton and its 1LO and 2LO peak energies with temperature in Fig. 7. As seen in this figure, the expected and the measured energy peak positions of the 1LO and 2LO replicas of the A-free exciton agree well, supporting our assignments. It is also noted that temperature variation of the A-free exciton peak energy follows the Varshni's[30] $E_g(T)=E_g(0)-\alpha T^2/(T+\beta)$ formula. A slight deviation is observed above 160 K due to the error in determination of the peak position resulting from temperature broadening and overlap with LO phonon replicas as explained before. A higher order LO phonon replica of the A free exciton also develops consistently with increasing temperature as seen in Fig. 6.

VIII. TIME-RESOLVED PL

TRPL is a nondestructive and powerful technique commonly used for the optical characterization of semiconductors. The exciton lifetime, an important parameter related to material quality and device performance, can be measured by TRPL spectroscopy. The efficiency of the radiative recombination is strongly related to decay time of the particular transition. As indicated before, the free excitonic features for the forming gas annealed ZnO sample were observed to be significantly stronger than the as-received sample. To understand the effects of postgrowth treatment, carrier recombination dynamics were measured for both samples at room temperature. The effects of excitation energy density were also explored.

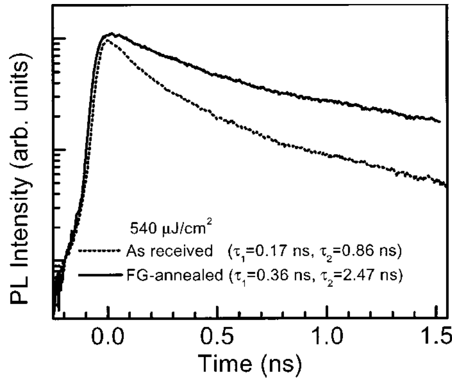

FIG. 8. Room temperature time resolved PL data for the as received and the FG treated samples.

Figure 8 shows the room temperature TRPL data at an excitation energy density of 540 $\mu J/cm^2$. The time-resolved signals were integrated over a 10 nm wide spectral region around the peak PL energy (3.266 eV). The instrument-limited rise implies that the relaxation processes to cool the carriers from 3.81 eV excitation energy-defined states to the zero momentum excitonic band edge states are very fast. For both samples, the decaying part of the TRPL data was well described by a biexponential decay function: $A_1 \exp(-t/\tau_1) + A_2 \exp(-t/\tau_2)$. Table III summarizes the decay constants and the amplitude ratios obtained from the fits.

The fast decay constant τ_1 is smaller for the as received sample, and most probably represents the effective nonradiative recombination at room temperature. The slow decaying component is attributed to the radiative lifetime of the free exciton. The 0.86 ns value measured for the as received sample is consistent with the 0.97 ns value measured by Koida *et al.*[31] for single crystal ZnO. In contrast, the recombination lifetimes of the Γ_5 and Γ_6 excitons at 2 K are reported as 259 and 245 ps, respectively, for bulk ZnO.[32] These faster recombination times may result from the efficient capture processes leading to bound excitons at low temperatures.[32] The relative magnitude of the slow decaying component to the fast decaying component ($A_2/A_1=0.094$ for 540 $\mu J/cm^2$) for the as received sample suggests dominant nonradiative processes, which may be governed by the defects introduced by the Zn vacancy complexes.[31]

After forming gas annealing the decay constants increased remarkably, and the slow decaying component became dominant ($A_2/A_1=2.54$ for 540 $\mu J/cm^2$), suggesting an increase in radiative recombination. This is also supported by the fact that the room temperature PL intensity increases by almost a factor of 4 in the forming gas annealed ZnO sample compared to the as received one. The increase in the decay times is clearly observed in Fig. 8.

When the excitation density is decreased from 540 to 54 $\mu J/cm^2$, the PL peak blueshifts by 15 meV. For the as received sample the decay constants increase slightly with increasing excitation density, whereas the forming gas treated sample follows an opposite trend. In addition, compared to the forming gas treated sample, the as received sample shows a more evident increase in the relative strength of the slow decaying component as the excitation density is increased, as the nonradiative centers begin to saturate.

In addition, the decay time constants of both as-received and forming gas annealed samples have been measured at 85 K. At this temperature, the main donor-bound exciton still dominates the overall cw-PL spectrum even though A- and B-free excitons are clearly observed. However, a distinction between the bound and the free excitons could not be made in the TRPL measurements due to resolution limitation of the spectrometer. Therefore, TRPL data reflect mainly the decay due to the main donor bound exciton. In order to measure purely the free excitonic emission decay time, the measurements had to be performed at temperatures above 160 K where the bound exciton emission diminishes.

The time constants measured at 85 K are also included in Table III for two different excitation densities. The main DBE emission has similar intensity for both samples as observed from the time-integrated and the cw PL. Compared to the as-received, the forming gas annealed sample showed slightly larger decay constants. Additionally, the decay times decreased with decreasing excitation energy density. In contrast to the significant improvement in free exciton lifetimes measured at room temperature, the postgrowth treatment is not observed to have a similar effect on the DBE decay times.

IX. CONCLUSIONS

We investigated the principal PL features in high quality ZnO substrate material and identified the intrinsic and extrinsic recombination lines. An A-free exciton binding energy of 60 meV was determined from the separation of the ground state and the excited state peak positions observed in the low

TABLE III. TRPL decay time constants and amplitude ratios for the ZnO samples at two different excitation energy densities. FX and DBE denote the free and donor bound excitons, respectively.

		540 $\mu J/cm^2$			54 $\mu J/cm^2$		
		τ_1 (ps)	τ_2 (ps)	A_2/A_1	τ_1 (ps)	τ_2 (ps)	A_2/A_1
300 K (*FX*)	As-received	170.4±1.8	863.9±14.8	0.094	116.5±1.5	585.0±6.4	0.060
	FG-annealed	358.7±8.8	2469±256	2.536	428.3±32.1	2969±15	2.476
85 K (DBE)	As-received	310.2±2.5	1130±6.6	0.653	286.8±2.9	1000±5.9	0.820
	FG-annealed	474.0±5.5	1285±15	0.614	366.4±4.1	1021±7.3	0.869

temperature PL spectra. Polariton features were also observed and discussed. The separation between bound exciton lines and their two electron transitions provided us the binding energies of the impurities present in the material. The localization energy of donor bound excitons has been explained in terms of the Hayne's rule. The controversial assignments of some peaks were also analyzed using their temperature evolutions. From the experimental data we aimed to clarify the peaks at 3.3724, 3.2898, 3.323, and 3.217 eV. From the energy separation between A- and B-free exciton transitions and also similarities between their temperature dependent PL intensities, the peak at 3.3724 eV was attributed to the B-free exciton bound to the main neutral donor. We also believe that the peaks at 3.2898 (and shoulders nearby) and 3.217 eV are related to the 1LO-phonon replicas of major neutral bound excitons and donor-acceptor pair transition, respectively, rather than the acceptor-bound excitons. Temperature dependent PL measurements reveal that the peak at 3.323 eV is related to the 2LO-phonon replica of the A-free exciton. This has been confirmed by the analysis of the peak energy shifts with temperature, and excellent agreement was realized with the expected trend in energy peak positions. However, the chemical origins of the observed peaks are still to be determined after further investigations.

Room temperature TRPL revealed a biexponential decay with decay constants 170 and 864 ps for the as received ZnO sample. Forming gas treatment is observed to increase these decay constants to 359 ps and 2.47 ns, respectively. This large increase in the recombination lifetimes and the relative increase in the strength of the slow decaying component suggest the improvement of the radiative recombination as well as a reduction in the nonradiative pathways.

ACKNOWLEDGMENTS

This work is funded by BMDO (monitored by C. W. Litton) and benefited from grants by ONR (monitored by C. E. C. Wood). In addition, the work at VCU benefited from grants by AFOSR (Dr. G. Witt and Dr. T. Steiner) and NSF (Dr. L. Hess and Dr. U. Varshney). H.O.E. gratefully acknowledges partial support from ARO and an AFOSR DURIP grant. The authors would like to thank Dr. C. Litton for long time encouragements and helpful discussions. The authors would like to thank M. A. Reshchikov for useful discussion throughout the course of this work. One of the authors, H.M., gratefully acknowledges many outstanding contributions to the field by Dr. D. C. Reynolds and Dr. C. W. Litton and many insightful discussions.

---

*Also at: Balıkesir University, Faculty of Arts & Sciences, Department of Physics, 10100 Balıkesir, Turkey.

†Also at: Atatürk University, Faculty of Arts & Sciences, Department of Physics, 25240 Erzurum, Turkey.

[1] Y. F. Chen, D. M. Bagnall, H. Koh, K. Park, K. Hiraga, Z. Zhu, and T. Yao, J. Appl. Phys. **84**, 3912 (1998).

[2] W. Y. Liang and A. D. Yoffe, Phys. Rev. Lett. **20**, 59 (1968).

[3] D. C. Reynolds, D. C. Look, B. Jogai, C. W. Litton, G. Cantwell, and W. C. Harsch, Phys. Rev. B **60**, 2340 (1999).

[4] D. C. Look, Mater. Sci. Eng., B **80**, 383 (2001).

[5] P. Zu, Z. K. Tang, G. K. L. Wong, M. Kawasaki, A. Ohtomo, H. Koinuma, and Y. Segawa, Solid State Commun. **103**, 459 (1997).

[6] D. M. Bagnall, Y. F. Chen, Z. Zhu, T. Yao, M. Y. Shen, and T. Goto, Appl. Phys. Lett. **73**, 1038 (1998).

[7] Y. W. Heo, S. J. Park, K. Ip, S. J. Pearton, and D. P. Norton, Appl. Phys. Lett. **83**, 63 (2003).

[8] K. K. Kim, H. S. Kim, D. K. Hwang, J. H. Lim, and S. J. Park, Appl. Phys. Lett. **83**, 1128 (2003).

[9] D. C. Reynolds, D. C. Look, B. Jogai, C. W. Litton, T. C. Collins, W. Harsch, and G. Cantwell, Phys. Rev. B **57**, 12 151 (1998).

[10] D. C. Reynolds, D. C. Look, B. Jogai, R. L. Jones, C. W. Litton, H. Harsch, and G. Cantwell, J. Lumin. **82**, 173 (1999).

[11] K. Thonke, Th. Gruber, N. Teofilov, R. Schönfelder, A. Waag, and R. Sauer, Physica B **308–310**, 945 (2001).

[12] C. Boemare, T. Monteiro, M. J. Soares, J. G. Guilherme, and E. Alves, Physica B **308–310**, 985 (2001).

[13] X. T. Zhang, Y. C. Liu, Z. Z. Zhi, J. Y. Zhang, Y. M. Lu, D. Z. Shen, W. Xu, X. W. Fan, and X. G. Kong, J. Lumin. **99**, 149 (2002).

[14] D. W. Hamby, D. A. Lucca, M. J. Klopfstein, and G. Cantwell, J. Appl. Phys. **93**, 3214 (2003).

[15] H. Alves, D. P. Sterer, A. Zeuner, T. Riemann, J. Christen, D. M. Hofmann, and B. K. Meyer, Opt. Mater. (Amsterdam, Neth.) **23**, 33 (2003).

[16] D. C. Reynolds, D. C. Look, B. Jogai, and T. C. Collins, Appl. Phys. Lett. **79**, 3794 (2001).

[17] A. Mang, K. Reimann, and St. Rübenacke, Solid State Commun. **94**, 251 (1995).

[18] D. G. Thomas, J. Phys. Chem. Solids **15**, 86 (1960).

[19] Y. S. Park, C. W. Litton, T. C. Collins, and D. C. Reynolds, Phys. Rev. **143**, 512 (1965).

[20] W. R. L. Lambrecht, A. V. Rodina, S. Limpijumnong, B. Segall, and B. K. Meyer, Phys. Rev. B **65**, 075207 (2002).

[21] J. J. Hopfield and D. G. Thomas, J. Phys. Chem. Solids **12**, 276 (1960).

[22] S. K. Suga, P. Cho, P. Heisinger, and T. Koda, J. Lumin. **12**, 109 (1967).

[23] C. Weisbuch and R. Ulbrich, Phys. Rev. Lett. **39**, 654 (1977).

[24] S. F. Chichibu, T. Sota, G. Cantwell, D. B. Eason, and C. W. Litton, J. Appl. Phys. **93**, 756 (2003).

[25] B. Monemar, J. P. Bergman, I. A. Buyanova, W. Li, H. Amano, and I. Akasaki, MRS Internet J. Nitride Semicond. Res. **1**, 2 (1996).

[26] Landolt/Bornstein, in *Numerical Data and Functional Relationship in Science and Technology*, New Series III Vol. 41B, edited by U. Rosler (Springer, Berlin, 1999).

[27] A. Kobayashi, O. F. Sankey, and J. D. Dow, Phys. Rev. B **28**, 946 (1983).

[28] J. Rarison, D. C. Herbert, D. J. Dean, and M. S. Skolnick, J. Phys. C **17**, 6483 (1984).

[29] A. K. Viswanath, J. I. Lee, S. Yu, D. Kim, Y. Choi, and C. H. Hong, J. Appl. Phys. **84**, 3848 (1998).

[30] Y. P. Varshni, Physica (Amsterdam) **34**, 149 (1967); L. Wang and N. C. Giles, J. Appl. Phys. **94**, 973 (2003).

[31] T. Koida, S. F. Chichibu, A. Uedono, A. Tsukazaki, M. Kawasaki, T. Sota, Y. Segawa, and H. Koinuma, Appl. Phys. Lett. **82**, 532 (2003).

[32] D. C. Reynolds, D. C. Look, B. Jogai, J. E. Hoelscher, R. E. Sherriff, M. T. Harris, and M. J. Callahan, J. Appl. Phys. **88**, 2152 (2000).